Electrochemical Capacitances of a Nanowire-Structured MnO $_2$ in Polyacrylate-Based Gel Electrolytes

Ho-Seong Nam, Nae-Lih Wu, Kuang-Tsin Lee, Kwang Man Kim, Chul Gi Yeom, Lovely Rose Hepowit, Jang Myoun Ko and Jong-Duk Kim

Email alerting service	Receive free email alerts when new articles cite this article - sign up in the box at the top right corner of the article or click here

Electrochemical Capacitances of a Nanowire-Structured MnO$_2$ in Polyacrylate-Based Gel Electrolytes

Ho-Seong Nam,[a] **Nae-Lih Wu,**[b,*] **Kuang-Tsin Lee,**[b] **Kwang Man Kim,**[c,*] **Chul Gi Yeom,**[d] **Lovely Rose Hepowit,**[d] **Jang Myoun Ko,**[d,z] **and Jong-Duk Kim**[a]

[a]*Center for Ultramicrochemical Process System, Department of Chemical and Biomolecular Engineering, Korea Advanced Institute of Science and Technology (KAIST), Daejon 305-701, Korea*
[b]*Department of Chemical Engineering, National Taiwan University, Taipei 106, Taiwan*
[c]*Research Team of Power Control Devices, Electronics and Telecommunications Research Institute (ETRI), Daejon 305-700, Korea*
[d]*Department of Applied Chemistry and Biotechnology, Hanbat National University, Daejon 305-719, Korea*

Nanowire-structured MnO$_2$ was synthesized by a sonochemical method and its electrochemical capacitances were investigated in three kinds of electrolytes: liquid-type KCl solution, potassium polyacrylate (PAAK), and potassium polyacrylate-*co*-polyacrylamide (PAAK-PAAM) gel polymer electrolytes (GPEs). The prepared MnO$_2$ with a nanowire structure had a high specific surface area and narrow pore distribution, which was very useful for gel-type electrolyte in supercapacitor applications. The specific capacitance of nanowire-structured MnO$_2$ with PAAK electrolyte exceeded 484 F g^{-1} at the conventional loading weight of MnO$_2$ (1.02 mg cm^{-2}) in the electrode. The nanowire-structured MnO$_2$ with PAAK electrolytes was a very promising electrode material for high-performance supercapacitors.
© 2012 The Electrochemical Society. [DOI: 10.1149/2.112206jes] All rights reserved.

Electrochemical capacitors are expected to be useful for high power applications due to their high-power capability; low sensitivity to temperature and easily monitored electrical behavior because they can fully discharge in a few seconds; longer cycles of several hundred thousand times; and high energy efficiency of charge and discharge.[1] Among the metal oxide active materials, amorphous MnO$_2$ has been drawing tremendous attention because of its low cost, natural abundance, and environmental safety.[2,3] However, the specific capacitance of MnO$_2$ depends on its particle size, morphology, and crystal structure because the MnO$_2$ usually has low intrinsically electronic conductivity and clustered morphology.[4] For a conventional MnO$_2$ electrode in an alkaline chloride electrolyte, the usual specific capacitance ranges from 100 to 200 F g^{-1}. At a low loading weight of MnO$_2$ in the electrode, however, the specific capacitance achieves a value greater than 300 F g^{-1}; for instance, 350 F g^{-1} for 0.05 mg cm^{-2} and 678 F g^{-1} for 0.00105 mg cm^{-2}.[5,6] Such a difference is likely due to the electrolyte accessibility to the active materials because amorphous MnO$_2$ is difficult to be completely wetted by the electrolyte. In this stage, the nanostructured MnO$_2$ employed in the supercapacitor electrode can be a critical issue in increasing its performance.[7,8] In particular, one-dimensional nanowire-structured MnO$_2$ has been proven to provide a high specific area, short diffusion path in the electrode, and good porous structures for electrolyte penetration. Subramanian et al.[9] hydrothermally prepared manganese dioxide (MnO$_2$) nanostructures that had a specific capacitance of 168 F g^{-1}. Jiang et al.[10] synthesized nanostrucutred MnO$_2$ by co-precipitation in the presence of Pluronic P123 and recorded a specific capacitance of 176 F g^{-1}. In addition, liquid-type electrolytes can be replaced with solid or gel-type electrolytes to prohibit the leakage and corrosion of liquid electrolytes and also to enhance the safety and reliability of the cell.[11]

In the present work, the nanowire-structured MnO$_2$ electrode is prepared by a sonochemical method to enhance the wettability of gel electrolytes and maintain a conventional MnO$_2$ loading weight (1.02 mg cm^{-2}).[12] The supercapacitive properties of the nanowire-structured MnO$_2$ electrode are investigated by cyclic voltammetry in different electrolyte systems: liquid-type KCl electrolyte, potassium polyacrylate (PAAK)-based gel polymer electrolyte (GPE), and potassium polyacrylate-*co*-polyacrylamide (PAAK-PAAM) GPE. The results are also compared with the previous reports[6,11] using the hydrous MnO$_2$ and similar electrolyte systems.

Experimental

Amorphous MnO$_2$ was synthesized by the method of Lee and Goodenough.[3] First, 0.55 g of manganese acetate (Aldrich) was dissolved in 40 mL of distilled water; 0.237 g of potassium permanganate (Aldrich) was dissolved in 15 mL of distilled water. The as-prepared potassium permanganate solution was then added dropwise to the manganese acetate solution using a syringe pump; ammonium hydroxide was added in the same manner under ultrasound irradiation with a 37 kHz ultrasonic wave at 600 W output power from a bath-type sonicator (Sonics & Materials, Danbury). During the sonication, the glass vessel was cooled with flowing water. After sonication for 30 min, the resulting brown precipitate was separated by decanting and washing several times with distilled water. It was subsequently dried at 40°C in a vacuum for 12 h to yield the nanowire-structured MnO$_2$. The as-prepared MnO$_2$ was characterized by a crystalline property analysis using an X-ray diffractometer (Siemens), morphology observations using a field emission scanning electron microscopy (FE-SEM, Nova 230, FEI Comp.), a transmission electron microscopy (FE-TEM) and selected electron diffraction patterns (JEM–2100F at 200 kV, JEOL). The specific surface area and the pore size distribution of the as-prepared MnO$_2$ were also measured by Brunauer-Emmett-Teller (BET) and Barrett-Joyner-Halenda (BJH) techniques, respectively, using a Smartsorb-92/93 (Micromeritics) after degassing at 100°C for 2 h.

A viscous slurry containing the as-prepared MnO$_2$ powder (59.5 wt%) as an active material, carbon black (Vulcan XC72) (25.5 wt%) as a conductive agent, poly(vinylidene difluoride) (Aldrich) (15 wt%) as a binder and *N*-methyl-2-pyrrolidone (Mitsubishi Chemical) as a solvent was pasted onto a Ti foil and dried at 120°C for 6 h in a vacuum oven. The dried electrode after the pressing process was cut to 1 cm × 1 cm dimension with a thickness of 116 μm, which contained 1.02 (±0.03) mg of the MnO$_2$. The theoretical density of the electrode was calculated to about 2.995 g cm^{-3} from the theoretical densities of all the components in the electrode, i.e., 5.026, 1.95, and 1.77 g cm^{-3}, corresponding to the MnO$_2$, carbon black, and binder, respectively. The packing density was also estimated by considering the loading weight and film thickness to 1.094 g cm^{-3}. The porosity of the nanowire-structured MnO$_2$ was then calculated as 40% from the electrode and packing densities. However, the electrode containing the conventional particles of MnO$_2$, having the thickness of 95 μm at the same composition and loading weight, showed the packing density of 2.285 g cm^{-3} and the porosity of 23.7%. The base polymers used to make GPE systems were PAAK (Aldrich) and

*Electrochemical Society Active Member.
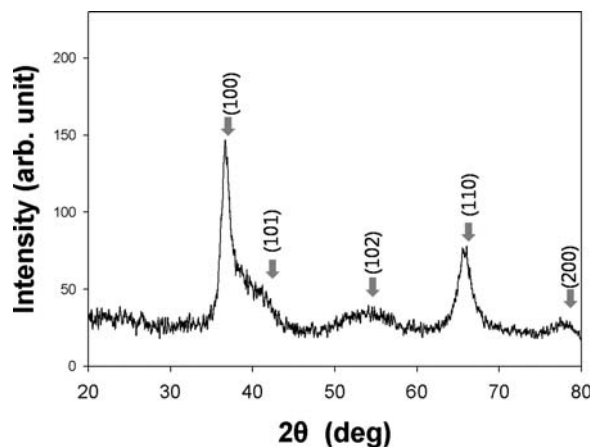[z]E-mail: jmko@hanbat.ac.kr.

Figure 1. X-ray diffraction pattern of the nanowire-structured MnO₂.

Figure 2. (a) FE-SEM, (b) FE-TEM images of the conventional MnO₂ without the sonochemical method, (c) FE-SEM, and (d) FE-TEM images of nanowire-structured MnO₂. The inset shows the selected electron diffraction pattern.

PAAK-PAAM (Aldrich). For electrochemical characterizations, the dried electrode was first immersed in a 10 cm³ solution of 1 M KCl, and 1 g of polymer was subsequently added into the solution. The concentration of KCl decreased slightly by the addition of polymer to become the GPE. The resulting self-supported GPE consisted of 9 wt% polymer, 6.7 wt% KCl, and 84.3 wt% H₂O.

Cyclic voltammetry was conducted with an electrochemical analyzer (Eco Chemie P/Gstat 30, Autolab), carried out in a single compartment with a three-electrode cell, and the distance between the working and the counter electrodes was about 1 cm and the reference electrode was Ag/AgCl saturated KCl (EG&G, 197 mV vs SHE at 25°C). The cyclic voltammetry was conducted in a voltage range from 0.1 to 0.9 V to the reduction and oxidation of active materials, but not of the electrolyte. The electrochemical window of ~0.8 V is electrochemically stable voltage range for all electrolytes adopted in this study. The specific capacitance (C_{sp}) was calculated from the cyclic voltammogram according to the equation of $C_{sp} = (q_a-q_c)/2m\Delta V$, where the q_a, q_c, m, and ΔV denote the anodic and cathodic charges, the mass of the active material, and the potential window of cyclic voltammetry, respectively. A chronopotential charge-discharge test was also performed between 0.1–0.9 V at the current densities of 1–3 A g⁻¹. The electrochemical impedance spectra were obtained from a frequency response analyzer (Eco Chemie P/Gstat 30, Autolab) with a frequency range of 10⁻¹-10⁵ Hz and a bias voltage of 10 mV. The room-temperature ionic conductivity (σ) of the electrolyte was calculated from the impedance spectrum according to the equation of $\sigma = l/(R_s \cdot A)$, where l was the distance (3 mm) between the reference and working electrodes and A the surface area (1 cm²) of the electrode.

Results and Discussion

Fig. 1 shows the X-ray diffraction pattern of the as-prepared MnO₂. The diffraction peaks of 2θ = 37.1, 42.4, 56.0, 68.8, and 78.9° correspond to the crystalline planes of (100), (101), (102), (110), and (200), respectively, in the amorphous α-MnO₂ structure (JCPDS no. 44-0141). The shapes and distribution of the MnO₂ particles can be confirmed by FE-SEM and FE-TEM images, as shown in Fig. 2. Conventional MnO₂ prepared without the sonochemical method has a spherical structure with a diameter of about 40 nm (see Figs. 2a and 2b).[10] The as-prepared MnO₂, however, has a nanowire structure composed of one-dimensional nanoarrays with a length of 300–700 nm a diameter of about 10 nm (L/D = 30–70). Meanwhile, there are some defects among the nanowires, which increased specific surface area. The corresponding selected area electron diffraction pattern also shows a faint ring image reflecting the amorphous structure of MnO₂ (see Figs. 2c and 2d). Thus, the nanowire-structured MnO₂ behaves as one-dimensional nanoarrays interconnected in a disorderly way, facilitating the electrolyte to penetrate the electrode more easily.
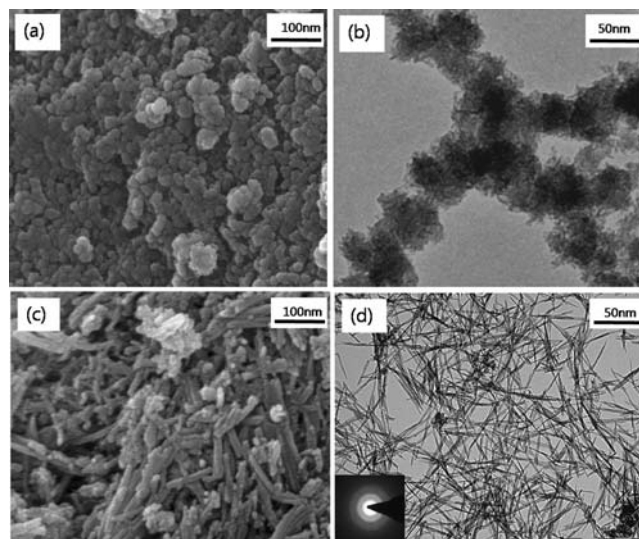
The porous properties of the MnO₂ electrode can be significant from the viewpoint of allowing the electrolyte into the pores within the electrode. As a porous property, Fig. 3 shows the N₂ adsorption/desorption isotherm of the nanowire-structured MnO₂. The N₂ sorption isotherm of the nanowire-structured MnO₂ shows an increase/decrease in an adsorption/desorption curve, which represents a uniform pore size or a narrow pore-size distribution[13] by the condensation of the porous architecture produced by the sonochemical method. To further understand the relationship between the microstructure of porous membrane and N₂ sorption isotherms, a decent textbook[14] can be referred. For the other porous properties, the BET surface area of the nanowire-structured MnO₂ is estimated to 250 m² g⁻¹. The BJH pore size distribution is also shown in the inset of Fig. 3. The pore is confirmed as a single modal type centered at around an average diameter of 3.6 nm, implying that the porous nanowire structure is facilitating the solvated ion transfer into the electrode up to a conventional loading weight (1.02 mg cm²) of the active material.

The supercapacitive properties of nanowire-structured MnO₂ are investigated by cyclic voltammetry between 0.1 and 0.9 V (vs. Ag/AgCl) in different electrolytes, i.e., liquid electrolyte, PAAK, and PAAK-PAAM based GPEs (see Fig. 4). Using the liquid-type KCl
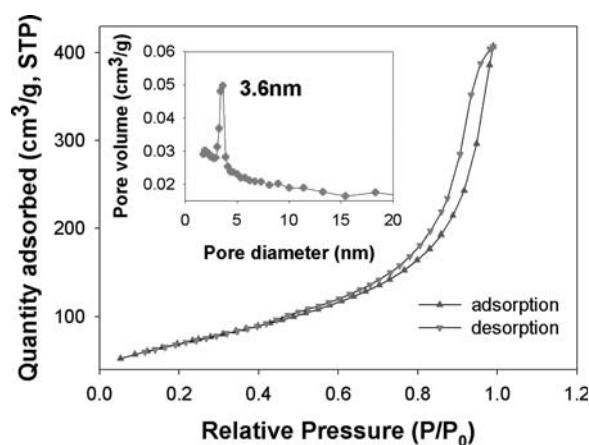

Figure 3. N₂ adsorption-desorption isotherms of the nanowire-structured MnO₂. The inset indicates the pore size distribution of the nanowire-structured MnO₂.
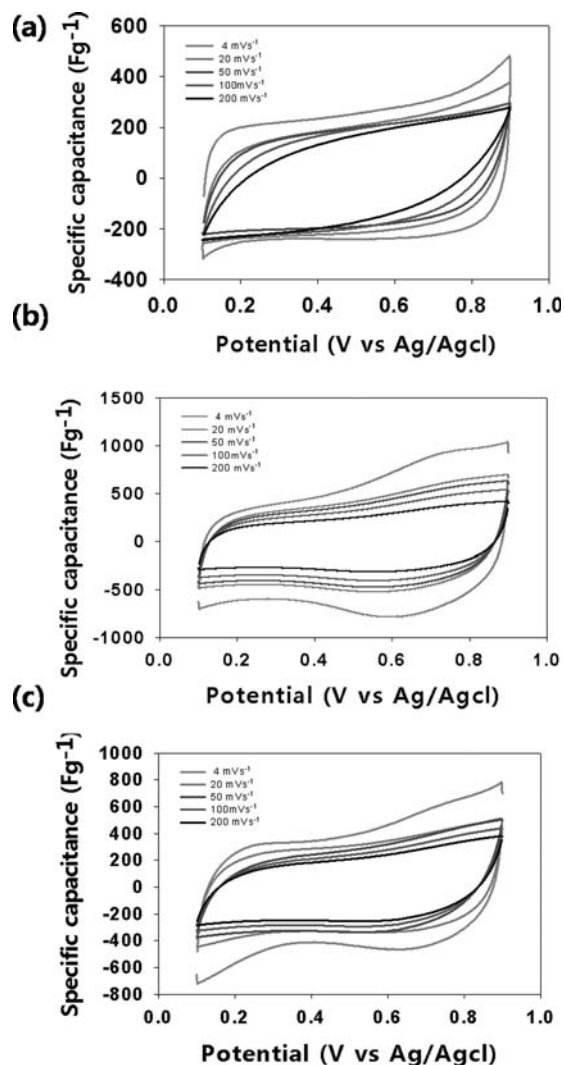
Figure 5. Specific capacitance of the nanowire-structured MnO_2 cells at various scan rates.

electrolyte cell, 92% for the PAAK cell, and 62% for the PAA-PAAM cells, compared with the hydrous MnO_2 particles. In addition, Fig. 5 shows that the capacitance decreasing rates of GPEs with increasing scan rate are higher than that of liquid electrolyte.

Fig. 6 shows the charge–discharge behavior of the nanowire-structured MnO_2 in the different electrolytes at the higher current

Figure 4. Cyclic voltammograms of the nanowire-structured MnO_2 cells with (a) the liquid-type KCl electrolyte, (b) the PAAK GPE, and (C) the PAAK-PAAM GPE. The salt concentration in the liquid electrolyte is 1 M KCl.

electrolyte, the cyclic voltammogram shows nearly rectangular profiles, indicating nearly ideal capacitor behavior.[15] Using GPEs, however, somewhat deviated cyclic voltammograms from the rectangular shape with high specific capacitances are obtained, especially in the low scan rate region. This is because of the nanowire-structured MnO_2 in which the GPE components containing the carboxylate groups easily penetrate the porous architecture of the MnO_2 which make it possible to further increase the interfacial contact between the electrode and the electrolyte. Thus, it is likely that the specific capacitance can be greatly enhanced by the adoption of polyacrylate-based GPE systems, as shown in Fig. 5. The cells composed of nanowire-structured MnO_2 and GPEs show higher specific capacitance than the liquid-electrolyte cell. Of these, the electrode with the PAAK electrolyte records the highest values of specific capacitance. For instance, at a scan rate of 4 mV s^{-1}, the nanowire-structured MnO_2 achieves 250 F g^{-1} in the liquid-type KCl, 485 F g^{-1} in the PAAK, and 380 F g^{-1} in the PAAK-PAAM electrolytes. There is a 94% and 52% increases in specific capacitance for the PAAK and PAAK-PAAM GPE cells, respectively, compared with the liquid electrolyte cell. In contrast, hydrous MnO_2 particles with the same electrolyte systems[6] shows that the maximum specific capacitances of 154, 253, and 235 F g^{-1}, were obtained at 4 mV s^{-1} for liquid-type KCl, PAAK, and PAAK-PAAM electrolytes, respectively. Thus, the nanowire-structured MnO_2 in the present study enhances the specific capacitance by 62% for the liquid
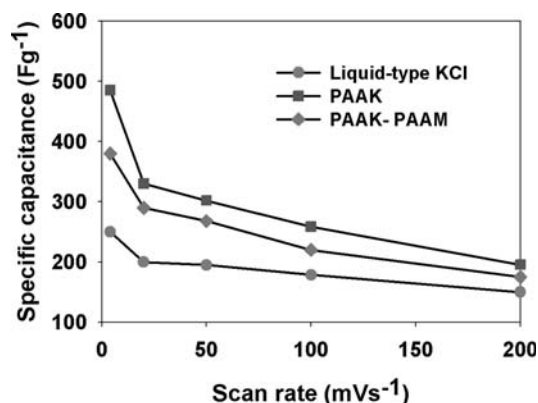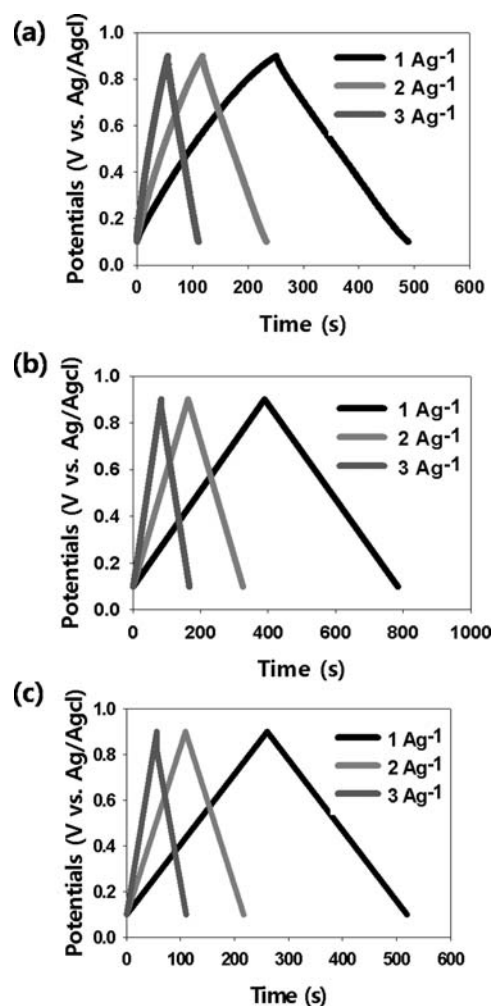

Figure 6. Chronopotential charge-discharge curves of the nanowire-structured MnO_2 under different current densities (1–3 A g^{-1}) in (a) the liquid-type KCl electrolyte, (b) the PAAK GPE, and (c) the PAAK-PAAM GPE. The salt concentration in the liquid electrolyte is 1 M KCl.
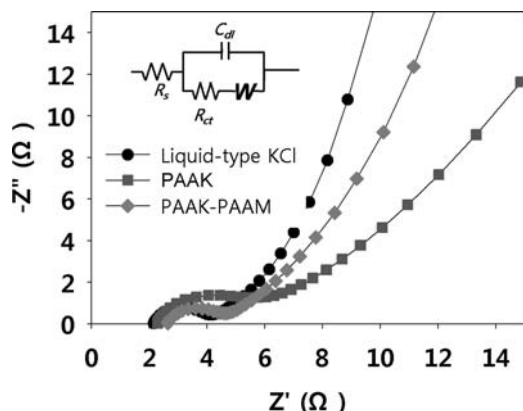
Figure 7. Nyquist plots of the nanowire-structured MnO$_2$ cells in the range of 10^{-1}–10^5 Hz at the bias potential of 10 mV.
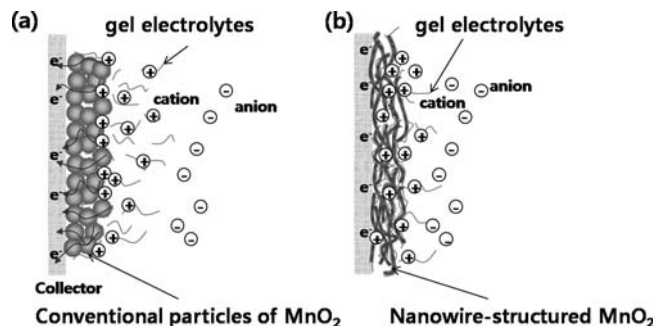

Figure 8. Schematic illustration of electrode layer between electrode and gel electrolyte in (a) the conventional MnO$_2$ and (b) the nanowire-structured MnO$_2$.

density range of 1–3 A g^{-1}. The charge-discharge curves are very symmetric but their slopes maintain the constant value, independent on the potential. These results indicate that the nanowire-structured MnO$_2$ electrodes in different electrolytes possess ideal capacitive behaviors in the higher current density range.

The electrochemical impedance spectra (see Fig. 7) of the nanowire-structured MnO$_2$ electrodes in the different electrolytes consist of partially overlapped semicircles followed by straight lines with a slope, which can be fitted by an equivalent circuit shown in the inset of Fig. 7. The plot consists of the Warburg impedance (W), solution resistance (R_s), charge transfer resistance (R_{ct}), and double-layer capacitance (C_{dl}).[16] The R_s is generally indicated by the first intersection of the semi-circle with the real Z'-axis. The W corresponds to the ion-diffusion effect on the interface between the active material and electrolyte, typically revealed by a straight line with a slope at the low frequency region. The R_{ct} indicates the faradaic interfacial charge transfer resistance, corresponding to the diameter of the semicircle at the high frequency region. Table I summarizes those impedance property values such as σ, R_s and R_{ct} of sample cells. The σ of a GPE system depends on the mobility of polymer chain in the electrolytes. Accordingly, the trend of the σ values is in the order of PAA-PAAM < PAAK < liquid electrolyte. PAAK-PAAM is more rigid, less flexible, and has a higher molecular weight than those of PAAK. Thus, the electrolyte containing more rigid and less flexible molecules has lower σ value than the less rigid and more flexible molecules. This agrees well with the results of Lee et al.[9] using hydrous MnO$_2$ particles synthesized by a conventional precipitation method. The σ of electrolytes mainly affects the electrochemical performance, especially R_s. If the σ of electrolytes is too low, it deteriorates the efficiency of the charge and discharge at high scan rates. Thus, the specific capacitances of PAAK and PAAK-PAAM, having a lower σ than liquid electrolyte, are rapidly decreased at higher scan rates than that of liquid electrolyte.

In the present study, the R_{ct} of the PAAK and PAAK-PAAM are higher than that of the liquid electrolyte because of the strong adsorption of the carboxylate group in the gel electrolytes on the MnO$_2$ surfaces over a wide range of pH. Within the pH range 5.2–7.2, the surface of MnO$_2$ is negatively charged (isoelectric point of pH$\sim$4.0), while the carboxylic groups in PAAK are dissociated. The interaction

between the surface of MnO$_2$ and the gel electrolyte is not electrostatic in nature but probably has specific interactions, e.g., hydrogen bond and complexes between Mn atoms and carboxyl groups.[17,18] Also, Lee at al.[6] proved by analyzing X-ray absorption near edge spectroscopy that the PAAK adsorbed on the MnO$_2$ surface. Thus, the gel electrolyte strongly adsorbed on the surface of the nanowire-structured MnO$_2$ is expected to play an important role of capacitance enhancement. There are two mechanisms proposed for the charge storage in MnO$_2$. The first is intercalation or deintercalation of alkali cations (K$^+$) in the electrolyte according to the reaction of MnO$_2$ + K$^+$ + e$^-$ $\leftrightarrow$ MnOOK. The second is the adsorption or desorption of alkali cations in the electrolyte on the MnO$_2$ according to the reaction of (MnO$_2$)$_{surface}$ + K$^+$ + e$^-$ $\leftrightarrow$ (MnO$_2$-K$^+$)$_{surface}$. Thus, the cation transfer between the electrolyte and the MnO$_2$ surface is a very important factor in obtaining a high capacitance.[9,19]

Comprehensively considering the results above, a mechanistic geometry for the nanowire-structured MnO$_2$ adopting the PAAK-based GPEs can be suggested, as shown in Fig. 8b. In the electrode containing conventional particles of MnO$_2$, the gel electrolyte hardly penetrates into the electrode layer because it is obviously more viscous and less mobile than that of liquid electrolyte. Accordingly, the presence of the cationic functional groups is expected not to be efficiently adsorbed at the surface of MnO$_2$ in the electrode with the conventional loading weight of MnO$_2$, i.e., 1.02 mg cm^{-2}. Thus, in the gel type electrode, the permeability of the electrolyte into the electrode does play an important role in the adsorption or desorption of cations in the electrolyte on the surface of MnO$_2$. However, the nanowire-structured MnO$_2$ electrode has plenty of space for efficient penetration of gel electrolytes into the electrode (see Fig. 8b). Thus, it could be that PAAK-based gel electrolytes are efficiently adsorbed on the electrode layer composed of the nanowire-structured MnO$_2$, which stores the charges by means of adsorption/desorption than intercalation/deintercalation to increase the capacitance.

Conclusions

In summary, the supercapacitive properties of nanowire-structured MnO$_2$ in the PAAK and PAAK-PAAM GPEs are characterized. The nanowire-structured MnO$_2$ electrode with PAAK GPE shows a maximum specific capacitance of 485 F g^{-1} at a low scan rate, which is much higher than that of the conventional MnO$_2$ electrode. Thus, this study confirms that the cell composed of nanowire-structured MnO$_2$ is even more suitable for the PAAK-based GPE for supercapacitor applications.

Table I. pH values and impedance properties of the nanowire-structured MnO$_2$ in various electrolytes.

Electrolyte system	pH	R_s (Ω)	R_{ct} (Ω)	σ (S cm^{-1})
Liquid-type KCl	6.2	2.16	2.13	0.139
PAAK GPE	5.2	2.30	3.86	0.130
PAAK-PAAM GPE	7.2	2.63	2.02	0.114

References

1. W. Dong, D. R. Rolison, and B. Dunn, *Electrochem. Solid-State Lett.*, **3**, 457 (2000).
2. M. Toupin, T. Brousse, and D. Bélanger, *Chem. Mater.*, **14**, 3946 (2002).
3. H. Y. Lee and J. B. Goodenough, *J. Solid State Chem.*, **144**, 220 (1999).
4. S. Devaraj and N. Munichandraiah, *Electrochem. Solid-State Lett.*, **8**, A373 (2005).
5. K.-T. Lee, C.-B. Tsai, W.-H. Ho, and N.-L. Wu, *Electrochem. Commun.*, **12**, 886 (2010).
6. K.-T. Lee, J.-F. Lee, and N.-L. Wu, *Electrochim. Acta*, **54**, 6148 (2009).
7. H. Y. Lee, S. W. Kim, and H. Y. Lee, *Electrochem. Solid-State Lett.*, **4**, A19 (2001).
8. J.-K. Chang and W.-T. Tsai, *J. Electrochem. Soc.*, **150**, A1333 (2003).
9. V. Subramanian, H. Zhu, and B. Wei, *J. Power Sources*, **159**, 361 (2006).
10. R. Jiang, T. Huang, J. Liu, J. Zhang, and A. Yu, *Electrochim. Acta*, **54**, 3047 (2009).
11. K.-T. Lee and N.-L. Wu, *J. Power Sources*, **179**, 430 (2008).
12. H.-S. Nam, J. K. Yoon, J. M. Ko, and J. D. Kim, *Mater. Chem. Phys.*, **123**, 331 (2010).
13. J. Y. Song, C. L. Cheng, Y. Y. Wang, and C. C. Wan, *J. Electrochem. Soc.*, **149**, A1230 (2002).
14. S. Lowell and J. E. Shields, *Powder Surface Area and Porosity*, 3rd Ed., Chapman & Hall (1991) Chap. 8.
15. C. L. Xua, S. J. Bao, L. B. Kong, H. Li, and H. L. Li, *J. Solid State Chem.*, **179**, 1351 (2006).
16. B. E. Conway, *Electrochemical Supercapacitors: Scientific Fundamentals and Technological Applications*, Plenum (1999).
17. S. Chibowski, E. Grzadka, and J. Patkowski, *Colloids Surf. A*, **326**, 191 (2008).
18. D. Solberg and L. Wågberg, *Colloids Surf. A*, **219**, 161 (2003).
19. M. Toupin, T. Brousse, and D. Bélanger, *Chem. Mater.*, **16**, 3184 (2004).